Preprints of the 21st IFAC World Congress (Virtual)
Berlin, Germany, July 12-17, 2020

Disturbance Observer Based Control Design via Active Disturbance Rejection Control: A PMSM Example

M.A. Aguilar-Orduña * **E.W. Zurita-Bustamante** * **H. Sira-Ramírez** * **Z. Gao** **

* *CINVESTAV-IPN, Mexico City, Mexico (e-mail: mario.aguilaro@cinvestav.mx, ezurita@cinvestav.mx, hsira@cinvestav.mx)*
** *Center for Advanced Control Technologies, Cleveland State University, Cleveland, OH 44115, USA (e-mail: z.gao@csuohio.edu)*

Abstract: A new Disturbance Observer Based (DOB) controller design procedure is here obtained via a reinterpretation of the disturbance estimation scheme, present in the Extended State Observer (ESO) based Active Disturbance Rejection (ADR) control scheme. If the reinterpreted disturbance estimation process is explicitly used, now, in combination with an ADR controller, the overall total disturbance effects are substantially diminished in the feedback loop, beyond that achievable by ESO-based ADR control alone. The context is that of nonlinear differentially flat systems, simplified to Kronecker chains of integrations. A Permanent Magnet Synchronous Motor (PMSM) example is examined and its performance is assessed from an experimental setting.

Keywords: Active Disturbance Rejection Control, Disturbance Observer Based Control, Extended State Observer, Reduced Order ESO.

1. INTRODUCTION

Disturbance Observer Based control is a mature area of control engineering with numerous developments and application examples (see Li et al. (2014),Ohishi et al. (1987)), which has been extended to nonlinear, single-input and multi-variable, systems (see Chen (2004) and Chen et al. (2016)). The approach is highly reminiscent of ADR control schemes but definite connections have remained elusive (Wang et al. (2018)). In this article, in the context of simplified, perturbed, input-to-flat output models of differentially flat systems, we establish a definite connection of ADRC with DOB control scheme. The DOB scheme is naturally hidden in the ADR control scheme at the level of the disturbance estimation part of the ESO observer used in ADR control. Furthermore, we take advantage of this connection, to propose a control scheme with enhanced disturbance attenuation features.

In section II of this article, ADR control is revisited in the context of simplified, perturbed, input-output flat systems and Reduced Order Extended State Observer (ROESO) based ADR control. The isolation, in the frequency domain setting, of the disturbance estimation part of the ROESO leads, directly, to the traditional DOB scheme, in which all the customary elements are clearly present: namely, inverse nominal plant, simultaneous low pass filtering of the plant inverse and of the input, subtraction at the input level of the estimated disturbance, obtained from the two simultaneously filtered versions of the input signal. In the literature, the controller design part of the DOB control scheme has always been left as an independent design problem (Wang et al. (2019)). In section III, taking advantage of the disturbance attenuation features of the ROESO based ADR control, a combination of the naturally identified DOB scheme, and an additional ADR controller is proposed. The net result is that the ADR control scheme now further attenuates the residual disturbance remaining from the cancellation effort exercised by the explicit DOB estimation scheme. This feature, is clearly verified, in Section IV, via a simulation example which compares the Integral Square Error (ISE) performance of the output tracking error trajectory, for an ADR control scheme alone, with that of the combined DOB and ROESO based ADR control scheme. Section V describes the use of the proposed ROESO based ADR control and DOB combination for a PMSM system example. Section VI contains the experimental results including the performance evaluation of the proposed DOB-ADRC scheme in comparison with the ADRC control scheme alone. The conclusions and suggestions for further work are summarized in Section VII.

2. ACTIVE DISTURBANCE REJECTION CONTROL

Active Disturbance Rejection Control is a robust control scheme, whose main features entitle: 1) Controller design on the basis of a simplified perturbed system which groups all exogenous and endogenous perturbations into a single total disturbance term. 2) On-line approximate estimation, via an extended state observer, of the total disturbance affecting the plant and 3) approximate disturbance cancellation, via a feedback control action which explicitly includes the disturbance estimate. In this section we use, instead of an ESO, a Reduced Order Extended State Observer (ROESO). This simplifies, somewhat, the developments and establishes an equivalence between ROESO based ADRC, Average Sliding Mode Control and, for second order systems, with PID control using a “dirty derivative” term (see Sira-Ramírez et al. (2019)).

2.1 Reduced Order Extended State Observer based ADRC

Consider the following third-order, perturbed, pure integration system.

$$y^{(3)} = \beta \upsilon + \xi(t), \quad (1)$$

where β is a known scalar gain and $\xi(t)$ is a total perturbation input. The signal, $\xi(t)$, can contain exogenous and endogenous disturbances, effects of un-modeled dynamics and, possibly, parameter uncertainties. Only the input, υ, and the output, y, are measurable. Defining $\upsilon = u/\beta$ and substituing it in (1) we have:

$$y^{(3)} = u + \xi(t), \quad (2)$$

Suppose it is desired to follow a given smooth trajectory, y^*, and by defining u^* as the nominal control input, computed as ${y^*}^{(3)}$; the output tracking error $e_y = y - y^*$ is seen to satisfy:

$$e_y^{(3)} = \beta e_u + \xi(t) \quad (3)$$

where $e_u = u - u^*$. In state-space representation, the system can be written as:

$$\dot{e}_{y_1} = e_{y_2} \quad (4)$$
$$\dot{e}_{y_2} = e_{y_3} \quad (5)$$
$$\dot{e}_{y_3} = \beta e_u + \xi(t) \quad (6)$$
$$e_{y_1} = e_y \quad (7)$$

Assume for a moment that e_{y_2} is measurable, the ROESO is given by:

$$\dot{\widehat{e}}_{y_2} = \widehat{e}_{y_3} + \lambda_2 \left(e_{y_2} - \widehat{e}_{y_2}\right) \quad (8)$$
$$\dot{\widehat{e}}_{y_3} = \beta e_u + z + \lambda_1 \left(e_{y_2} - \widehat{e}_{y_2}\right) \quad (9)$$
$$\dot{z} = \lambda_0 \left(e_{y_2} - \widehat{e}_{y_2}\right) \quad (10)$$
$$e_{y_2} = \dot{e}_{y_1} = \dot{e}_y \quad (11)$$

where $\widehat{(\cdot)}$ are the estimations of the phase-variables and, z is the total disturbance estimation term. In practice, this scheme is not implementable due to the lack knowkledge of the flat output time derivatives; for this purpose, define the following variables:

$$\widehat{\zeta}_2 = \widehat{e}_{y_2} - \lambda_2 e_{y_1}, \ \widehat{\zeta}_3 = \widehat{e}_{y_3} - \lambda_1 e_{y_1}, \quad \widehat{\eta} = z - \lambda_0 e_{y_1} \quad (12)$$

Then, an implementable ROESO observer is written in terms of the new variables,

$$\dot{\widehat{\zeta}}_2 = \widehat{\zeta}_3 - \lambda_2 \widehat{\zeta}_2 + \left(\lambda_1 - \lambda_2^2\right) e_y \quad (13)$$
$$\dot{\widehat{\zeta}}_3 = \beta e_u + \widehat{\eta} - \lambda_1 \widehat{\zeta}_2 + \left(\lambda_0 - \lambda_1 \lambda_2\right) e_y \quad (14)$$
$$\dot{\widehat{\eta}} = -\lambda_0 \widehat{\zeta}_2 - \lambda_0 \lambda_2 e_y. \quad (15)$$

This observer yields the original phase-variables estimates of the tracking errors:

$$\widehat{e}_{y_2} = \widehat{\zeta}_2 + \lambda_2 e_y; \quad \widehat{e}_{y_3} = \widehat{\zeta}_3 + \lambda_1 e_y; \quad z = \widehat{\eta} + \lambda_0 e_y \quad (16)$$

The estimation errors of the tracking error phase variables, satisfy the following relations,

$$\tilde{e}_{y_2} = \zeta_2 - \widehat{\zeta}_2 = e_{y_2} - \widehat{e}_{y_2} \quad (17)$$
$$\tilde{e}_{y_3} = \zeta_3 - \widehat{\zeta}_3 = e_{y_3} - \widehat{e}_{y_3} \quad (18)$$
$$\tilde{e}_{\xi} = \eta - \widehat{\eta} = \xi - z \quad (19)$$

where:

$$\zeta_2 = e_{y_2} - \lambda_2 e_y, \quad \zeta_3 = e_{y_3} - \lambda_1 e_y, \quad \eta = \xi - \lambda_0 e_y. \quad (20)$$

Thus, one obtains the tracking error state and the disturbance estimation errors dynamics. Taking into account the relationships above, we get:

$$\frac{d}{dt}\tilde{e}_{y_2} = \tilde{e}_{y_3} - \lambda_2 \tilde{e}_{y_2} \quad (21)$$
$$\frac{d}{dt}\tilde{e}_{y_3} = \tilde{e}_{\xi} - \lambda_1 \tilde{e}_{y_2} \quad (22)$$
$$\frac{d}{dt}\tilde{e}_{\xi} = \dot{\xi} - \lambda_0 \tilde{e}_{y_2} \quad (23)$$

It follows that the ROESO estimation error dynamics is governed by:

$$\tilde{e}_{y_2}^{(3)} + \lambda_2 \ddot{\tilde{e}}_{y_2} + \lambda_1 \dot{\tilde{e}}_{y_2} + \lambda_0 \tilde{e}_{y_2} = \dot{\xi} \quad (24)$$

A proper choice of the design parameters would guarantee exponential asymptotic stability in the unperturbed system case. Select the design parameters, $\{\lambda_2, \lambda_1, \lambda_0\}$, in such a manner that they constitute a Hurwitz set. In the frequency domain, the transfer functions of the state and disturbance estimation errors are:

$$\tilde{e}_{y_2}(s) = \left[\frac{s}{s^3 + \lambda_2 s^2 + \lambda_1 s + \lambda_0}\right] \xi(s) \quad (25)$$
$$\tilde{e}_{y_3}(s) = (s + \lambda_2) e_{y_2} = \left[\frac{s(s + \lambda_2)}{s^3 + \lambda_2 s^2 + \lambda_1 s + \lambda_0}\right] \xi(s) \quad (26)$$
$$\tilde{e}_{\xi}(s) = s e_{y_3} + \lambda_1 e_{y_2} = \left[\frac{s\left(s^2 + \lambda_2 s + \lambda_1\right)}{s^3 + \lambda_2 s^2 + \lambda_1 s + \lambda_0}\right] \xi(s) \quad (27)$$

Using the estimations of the phase-variables and the total disturbance term, the proposed reduced-order extended state observer-based ADRC controller is written as,

$$e_u = \left(\frac{1}{\beta}\right)\left(-\gamma_2 \widehat{e}_{y_3} - \gamma_1 \widehat{e}_{y_2} - \gamma_0 e_y - z\right) \quad (28)$$

With a corresponding characteristic polynomial,

$$s^3 + \gamma_2 s^2 + \gamma_1 s + \gamma_0 \quad (29)$$

Again, a proper choice of parameters is made which guaranties asymptotic exponential stability of the unperturbed system. We select the design parameters $\{\gamma_2, \gamma_1, \gamma_0\}$ so that they form a Hurwitz set. This is achieved by a term by term identification of the third-order characteristic polynomial with a known third-order Hurwitz polynomial of the form: $(s^2 + 2\zeta\omega_n s + \omega_n^2)(s + p)$, $\zeta, \omega_n, p > 0$.

Notice that:

$$\widehat{e}_{y_3} = \widehat{\ddot{e}}_y = \ddot{e}_y - \tilde{e}_{y_3}, \ \widehat{e}_{y_2} = \widehat{\dot{e}}_y = \dot{e}_y - \tilde{e}_{y_2}, \ z = \xi - \tilde{e}_{\xi} \quad (30)$$

In the frequency domain, the closed loop system is described by:

$$\left(s^3 + \gamma_2 s^2 + \gamma_1 s + \gamma_0\right) e_y(s) = \gamma_2 \tilde{e}_{y_3}(s) + \gamma_1 \tilde{e}_{y_2}(s) + \tilde{e}_{\xi}(s) \quad (31)$$
$$= \left[\frac{s^3 + (\lambda_2 + \gamma_2) s^2 + (\lambda_1 + \lambda_2\gamma_2 + \gamma_1) s}{s^3 + \lambda_2 s^2 + \lambda_1 s + \lambda_0}\right] \xi(s) \quad (32)$$

Hence, the load sensitivity function for the closed-loop system, is expressed as:

$$e_y(s) = \left[\frac{s\left(s^2 + (\lambda_2 + \gamma_2) s + (\lambda_1 + \lambda_2\gamma_2 + \gamma_1)\right)}{(s^3 + \lambda_2 s^2 + \lambda_1 s + \lambda_0)(s^3 + \gamma_2 s^2 + \gamma_1 s + \gamma_0)}\right] \xi(s) \quad (33)$$

After some algebra, it is not difficult to see that the closed-loop transfer function relating, $\xi(s)$, and, $e_y(s)$, induced by the ROESO based ADRC controller, is of the form:

$$e_y(s)=\left[\frac{s\left(s^2+\kappa_5 s+\kappa_4\right)}{s^6+\kappa_5 s^5+\kappa_4 s^4+\kappa_3 s^3+\kappa_2 s^2+\kappa_1 s+\kappa_0}\right]\xi(s)\,, \quad (34)$$

where the transfer function coefficients $\kappa_5, \cdots, \kappa_0$, are obtained, in terms of the observer and controller design parameters, as,

$$\begin{aligned}
\lambda_2+\gamma_2 &= \kappa_5\\
\lambda_1+\lambda_2\gamma_2+\gamma_1 &= \kappa_4\\
\lambda_0+\lambda_1\gamma_2+\lambda_2\gamma_1+\gamma_0 &= \kappa_3\\
\lambda_0\gamma_2+\lambda_1\gamma_1+\lambda_2\gamma_0 &= \kappa_2\\
\lambda_0\gamma_1+\lambda_1\gamma_0+ &= \kappa_1\\
\lambda_0\gamma_0 &= \kappa_0
\end{aligned}$$

The corresponding transfer function of the ROESO based ADR controller is found to be:

$$C\left(s\right)=\frac{1}{\beta}\left[\frac{\kappa_3 s^3+\kappa_2 s^2+\kappa_1 s+\kappa_0}{s\left(s^2+\kappa_5 s+\kappa_4\right)}\right] \quad (35)$$

3. ADRC BASED DOB DESIGN

Consider the output reference trajectory tracking problem, in a third order perturbed flat plant as in (3)

$$e_y^{(3)}=\beta e_u+\xi\left(t\right)$$

A ROESO based ADRC control scheme leads to the following estimation errors transfer functions, excited by the perturbation input,

$$\tilde{e}_{y_2}\left(s\right)=\left[\frac{s}{s^3+\lambda_2 s^2+\lambda_1 s+\lambda_0}\right]\xi\left(s\right) \quad (36)$$

$$\tilde{e}_{\xi}\left(s\right)=\xi\left(s\right)-z(s)=\left[\frac{s\left(s^2+\lambda_2 s+\lambda_1\right)}{s^3+\lambda_2 s^2+\lambda_1 s+\lambda_0}\right]\xi\left(s\right) \quad (37)$$

From (37), the total disturbance estimation term can be represented as,

$$z(s)=\xi(s)-\tilde{e}_{\xi}(s)=\left[\frac{\lambda_0}{s^3+\lambda_2 s^2+\lambda_1 s+\lambda_0}\right]\xi\left(s\right) \quad (38)$$

Taking into account the Laplace transform of the perturbed third-order system, notice that $\xi(s) = s^3 e_y(s) - \beta e_u(s)$. It then follows that the estimation of the disturbance term is given by,

$$\begin{aligned}
z(s) &= \left[\frac{\lambda_0}{s^3+\lambda_2 s^2+\lambda_1 s+\lambda_0}\right]\left(s^3 e_y-\beta e_u\left(s\right)\right) &(39)\\
&= \left[\frac{s^3\lambda_0}{s^3+\lambda_2 s^2+\lambda_1 s+\lambda_0}\right]e_y &(40)\\
&\quad -\left[\frac{\lambda_0}{s^3+\lambda_2 s^2+\lambda_1 s+\lambda_0}\right]\beta e_u &(41)
\end{aligned}$$

The transfer functions above, represent, respectively, the inverse of the nominal plant multiplied by a low pass filter $Q(s)$,

$$Q\left(s\right)G^{(-1)}\left(s\right)=\left[\frac{s^3\lambda_0}{s^3+\lambda_2 s^2+\lambda_1 s+\lambda_0}\right]e_y \quad (42)$$

and the same low pass filter excited by the control input error:

$$Q\left(s\right)\beta e_u=\left[\frac{\lambda_0}{s^3+\lambda_2 s^2+\lambda_1 s+\lambda_0}\right]\beta e_u \quad (43)$$

which is, precisely, the traditional DOB estimation scheme for the additive uncertain perturbation [Chen et al. (2016); Ohishi et al. (1987)]. This disturbance estimate term is used as part of the feedback controller action to approximately cancel the effects of the total disturbance term.

4. SIMULATION STUDY

The ROESO ADRC controller, developed in section 2.1, is implemented in a third-order, perturbed, pure integration system (1) tracking a smooth reference trajectory for a rest to rest maneuver during a time interval of 3 seconds. The DOB observer, designed in section 3, is incorporated into the control scheme, as shown in figure 1. The effects of adding the DOB-disturbance estimation as part of the feedback control action, are depicted in the next graphs.

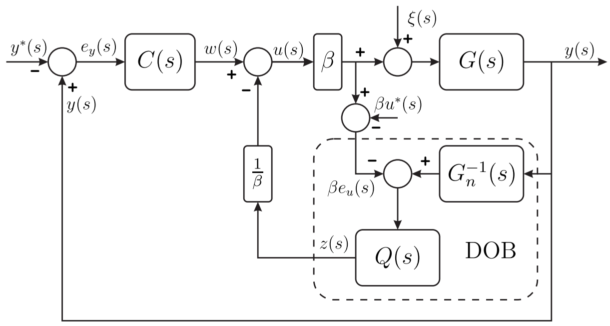

Fig. 1. ADRC-DOB control scheme

Figure 1 shows the proposed control scheme, which employs the DOB estimated disturbance, where $C(s)$ is the transfer function of the ROESO-ADRC controller (35), $G_n^{-1}(s)$ is the inverse of the unperturbed nominal plant, and $Q(s)$ the proposed low pass filter (43). Notice that this control scheme is a ROESO based ADRC controller assisted by a DOB observer; the influence of the DOB disturbance estimation can be eliminated by only taking it out of the diagram.

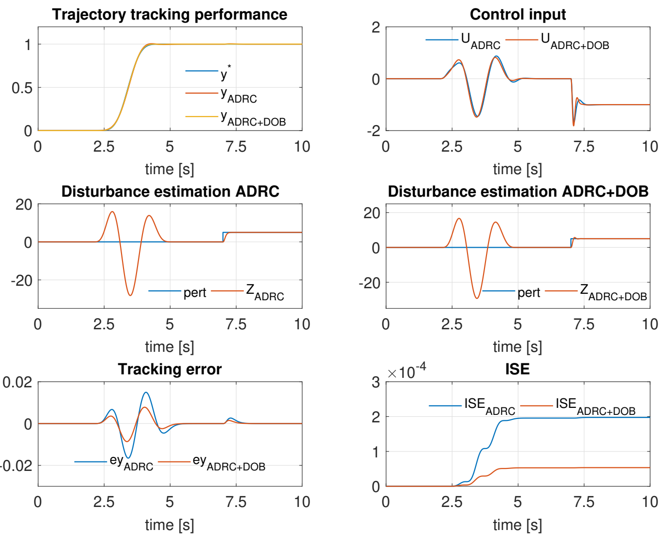

Fig. 2. Trajectory tracking with a step disturbance

Figure 2 and 3 depicts the simulation results of tracking a rest-to-rest maneuver. On figure 2, the system is disturbed with a 5 units step in $t = 7[s]$. While in figure 3, a time-variant disturbance signal perturbs the system all the time.

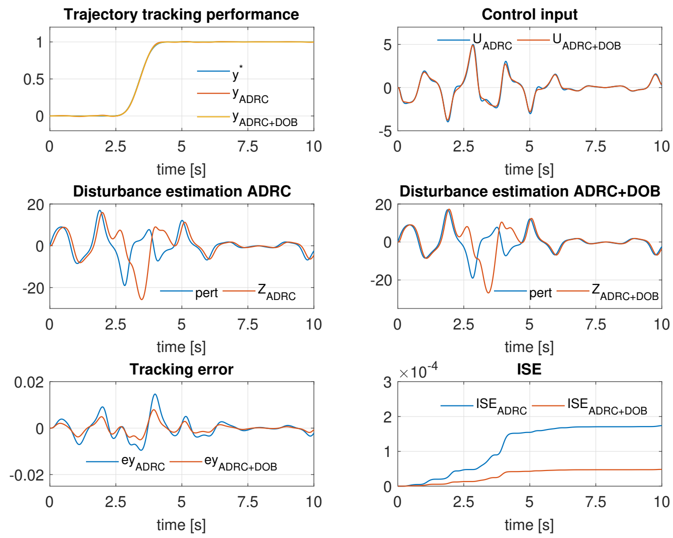

Fig. 3. Trajectory tracking with a time-varying perturbation

Despite the ROESO ADRC performs-well against disturbance signals, the tracking error graph shows quite an improvement when we include the DOB disturbance estimation term. However, integral square error indices were arranged in order to objectively compare the performance of both techniques; once again, a significant improvement is shown by the ISE index graph, incorporating the DOB scheme; as seen on the tracking error graphs in Fig. (2) and (3). This index is defined by,

$$ISE = \int_0^t (y - y^*(t))^2 dt \tag{44}$$

We compute the controller design parameters, $\{\gamma_2, \gamma_1, \gamma_0\}$, and the observer design parameters, $\{\lambda_2, \lambda_1, \lambda_0\}$, by using the following third-order Hurwitz polynomial:

$$(s^2 + 2\zeta_o \omega_{no} s + \omega_{no}^2)(s + p_o) \quad ROESO/DOB \tag{45}$$

$$(s^2 + 2\zeta \omega_n s + \omega_n^2)(s + p) \quad ADRC \tag{46}$$

Table 1 shows the parameters employed in this simulation.

Gain	ADRC			ROESO/DOB		
β	ω_n	ζ	p	ω_{no}	ζ_o	p_o
5	10	1	10	30	1	30

Table 1. Simulation parameters

5. A PERMANENT MAGNET SYNCHRONOUS MOTOR CONTROL APPLICATION

The set of differential equations describing the mathematical model of a PMSM, written in a *d*-*q* frame, is given by Chiasson (2005):

$$L_s \frac{di_d}{dt} = -R_s i_d + n_p \omega L_s i_q + u_d \tag{47}$$

$$L_s \frac{di_q}{dt} = -R_s i_q - (n_p L_s i_d + K_m)\omega + u_q \tag{48}$$

$$J \frac{d\omega}{dt} = K_m i_q - B\omega - \tau_L \tag{49}$$

where $\frac{d\theta}{dt} = \omega$, i_d and i_q are the phase currents, θ and ω represent, respectively, the angular position and the angular velocity. The variables u_d and u_q are the control input voltages, and τ_L is the unknown time-varying load torque. The parameter, R_s is the stator resistance, L_s is the stator inductance, J and B represent, respectively, the moment inertia and the rotational friction coefficient. The parameter $K_m i_q$ is the back-emf (back electro-motive force) term and, finally, n_p is the number of pole pairs.

5.1 ADRC and DOBC based ADRC

The mathematical model of the PMSM (47) is a nonlinear MIMO, differentially flat, system with two flat outputs given by i_d and θ (See Sira-Ramírez et al. (2017)). The simplified input-output perturbed model for the phase current i_d and for the angular position θ are given by,

$$\frac{di_d}{dt} = \frac{1}{L_s} u_d + \xi_i(t) \tag{50}$$

$$\frac{d^3\theta}{dt^3} = \frac{K_m}{JL_s} u_q + \xi_\theta(t) \tag{51}$$

where ξ_i and ξ_θ lump all the non included terms of the model, which are taken to represent the *total disturbances*, we have:

$$\xi_i(t) = -\frac{R_s}{L_s} i_d + n_p \omega i_q$$

$$\xi_\theta(t) = -\frac{R_s K_m}{JL_s} i_q + \frac{1}{JK_m}(\frac{K_m}{L_s} - n_p i_d)\omega + \frac{B}{J}\frac{d\omega}{dt} - \frac{1}{J}\dot{\tau}_L$$

To control the direct current i_d, we deal with a first order controlled system. For this, we propose a PI^2 (Proportional-Double Integral) control, written in "s" domain as,

$$u_d = u_d^* - L_s \left[\frac{k_2 s^2 + k_1 s + k_0}{s^2} \right] (i_d - i_d^*) \tag{52}$$

For the control of the angular position, θ, we have a third order controlled system. In this case, to avoid the measurements of the angular velocity and angular acceleration, and in accordance with section 2.1, we propose a ROESO in terms of the angular position reference trajectory tracking error,

$$\dot{\widehat{\zeta}}_2 = \widehat{\zeta}_3 - \lambda_2 \widehat{\zeta}_2 + \left(\lambda_1 - \lambda_2^2\right) e_\theta \tag{53}$$

$$\dot{\widehat{\zeta}}_3 = u + \widehat{\eta} - \lambda_1 \widehat{\zeta}_2 + (\lambda_0 - \lambda_1 \lambda_2) e_\theta \tag{54}$$

$$\dot{\widehat{\eta}} = -\lambda_0 \widehat{\zeta}_2 - \lambda_0 \lambda_2 e_\theta \tag{55}$$

where $e_\theta = \theta - \theta^*$. Defining, respectively, the first and second order time derivative of e_θ as, e_{y2} and e_{y3} respectively, their estimates are given by:

$$\widehat{e}_{y_2} = \widehat{\zeta}_2 + \lambda_2 e_y; \quad \widehat{e}_{y_3} = \widehat{\zeta}_3 + \lambda_1 e_y; \quad z = \widehat{\eta} + \lambda_0 e_y \tag{56}$$

The corresponding ADR control for the tracking of the angular position reference trajectory $\theta^*(t)$, using the ROESO, is just given by:

$$u_q = u^* - \frac{JL_s}{K_m} \left[-k_2 \widehat{e}_{y_3} - k_1 \widehat{e}_{y_2} - k_0 e_\theta - z \right] \tag{57}$$

The direct current is stabilized to zero (i.e., $i_d^* = 0$) [Sira-Ramírez et al. (2014)]. In closed loop, both closed loop sub-systems resemble a set of decoupled perturbed linear systems, while the state and input interactions are confined to the additive total disturbance signals (see Zurita-Bustamante et al. (2018)). The characteristic polynomial, associated with the closed loop of direct current control, is obtained as a third order polynomial. So, we compute the PI^2, ADR controllers, and the observer design parameters, by using the following third-order Hurwitz polynomials:

$$(s^2 + 2\zeta_1\omega_1 s + \omega_1^2)(s + p_1) \qquad PI^2 \qquad (58)$$

$$(s^2 + 2\zeta_2\omega_2 s + \omega_2^2)(s + p_2) \qquad ROESO \qquad (59)$$

$$(s^2 + 2\zeta_3\omega_3 s + \omega_3^2)(s + p_3) \qquad ADRC \qquad (60)$$

5.2 A DOBC based ADRC

Based on section 3, a DOB scheme is proposed by extracting it from the estimation part of the ADR control scheme. For the case of a third order system, the DOB scheme estimating the total disturbance is given by:

$$z = \xi - \tilde{e}_\xi = \left[\frac{\lambda_0}{s^3 + \lambda_2 s^2 + \lambda_1 s + \lambda_0}\right]\xi(s) \qquad (61)$$

$$= \left[\frac{\lambda_0}{s^3 + \lambda_2 s^2 + \lambda_1 s + \lambda_0}\right]\left(s^3 e_y - \beta e_u(s)\right) \qquad (62)$$

$$= \left[\frac{s^3\lambda_0}{s^3 + \lambda_2 s^2 + \lambda_1 s + \lambda_0}\right]e_y \qquad (63)$$

$$- \left[\frac{\lambda_0}{s^3 + \lambda_2 s^2 + \lambda_1 s + \lambda_0}\right]\beta e_u \qquad (64)$$

where the parameters $\lambda_0, \ldots, \lambda_2$ are taken from the ROESO design and $\beta = \frac{K_m}{JL_s}$.

6. EXPERIMENTAL SETUP

An experimental platform was developed for the control of the angular position in the PMSM. The parameter values of the motor are shown in Table 2. In figure 4, a block diagram of the built platform is depicted. This experimental setup is integrated by a three phase diode bridge rectifier, a 2.4 kW voltage source inverter and a Baldor PMSM. The PWM device (10 kHz), the Bézier polynomial, the *d-q/abc* transformation, and the ADRC and DOB-ADRC position tracking controller are implemented in the STM32F4 controller card. The sample period of the card was set to $10\mu s$.

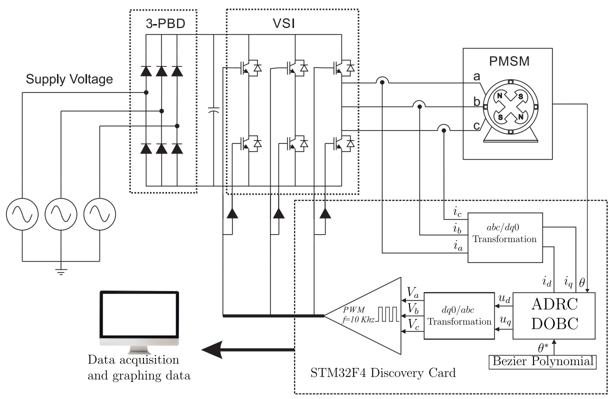

Fig. 4. Block diagram of the experimental setup for the trajectory tracking of angular position.

Table 2. Motor Parameters

Parameters	Value
R_s	$1.6[\Omega]$
L_s	$6.365[mH]$
$V_{pk}/krpm$	$77.4[V]$
Number of pole pairs n_p	2
Moment of inertia J	$0.182E{-}3[kg - m^2]$
Friction Coefficient B	$8.7E{-}5[kg - m^2/s]$

The parameters for the ROESO and for the feedback linear controller are shown in Table 3. A trajectory tracking task was developed to independently test the ADRC and DOBC-ADRC controllers. The initial angular position was set to 0 [rad] and the final desired angular position was set to 10π [rad] in the time-interval, [4 , 7] seconds. After this, the desired angular position smoothly goes back to 0 [rad] during the time interval: [10 , 13] seconds. Finally, the desired position was set to -10π [rad], based on an interpolation polynomial of the Bézier type, during the time interval: [16 , 19] seconds. In figure 5, the responses of, both, an active disturbance rejection control and an ADRC based DOBC are shown. Figure 5 depicts the angular position reference trajectory tracking performance, whose reference trajectory is also based on an interpolation polynomial of the Bezier type. The initial angular position was set to 0 [rad] and the final desired angular position was specified to 40π [rad]. The initial time was set to 1.5 seconds and the final time is 3.5 seconds. Figure 6 shows

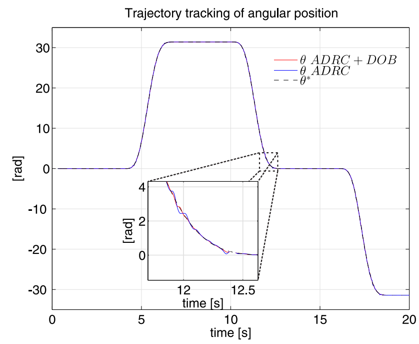

Fig. 5. Trajectory tracking performance for the ADRC and ADRC-DOB in the nonlinear PMSM.

PI^2		ROESO		ADRC	
Parameter	Value	Parameter	Value	Parameter	Value
ζ_1	1	ζ_2	1	ζ_3	1
ω_1	10	ω_2	450	ω_3	200
p_1	10	p_2	450	p_3	200

Table 3. Simulation parameters

the control input voltage u_d in the d_q frame. Also, the corresponding phase currents, i_d and i_q, are shown. The direct current is close to zero amperes, as desired.

Both control schemes, ADRC and DOBC-ADRC, present similar performances for the trajectory tracking task. However, ISE indices were arranged in order to objectively compare the performance of both techniques.

In figure 7 the behavior of the ISE indices are shown, for both control schemes. As it can be observed, the

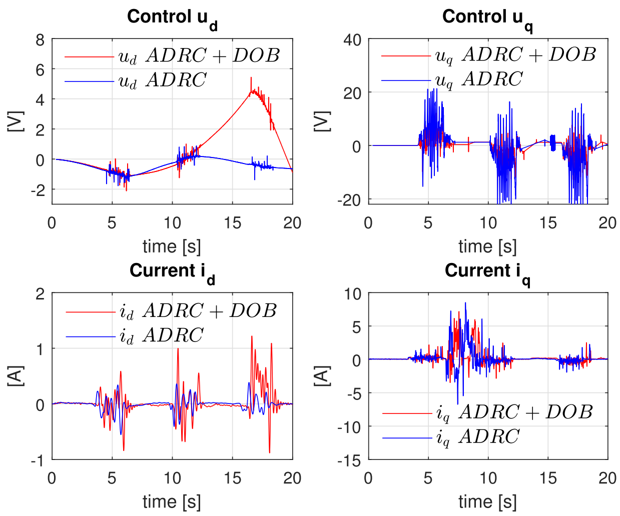

Fig. 6. Direct and quadrature voltage for the trajectory tracking of angular position with ADRC and DOBC-ADRC schemes.

DOB-ADR controller presents a substantially better performance than the ROESO based ADRC scheme alone. This is because, in the latter case, the control scheme is estimating, and attenuating, the residual disturbance obtained after subtracting, from the control input, its DOB estimate.

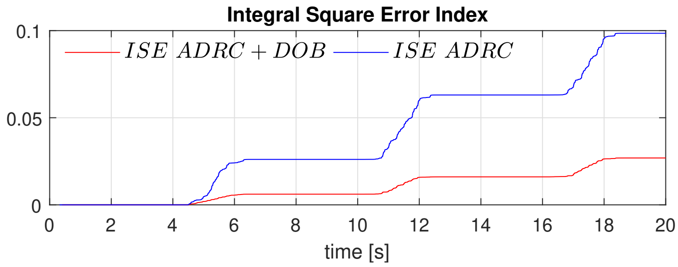

Fig. 7. ISE index comparing the performances of, both, the ADRC and the DOB-ADRC schemes.

7. CONCLUSIONS

This paper combines Disturbance Observer Based (DOB) control with Extended State Observer (ESO) based Active Disturbance Rejection (ADR) control. Using a frequency domain framework, for describing the disturbance estimation part of the (ROESO based ADR control), simple algebraic manipulations demonstrate that the total disturbance observation part, of the DOB scheme, is naturally obtained from the ROESO subsystem, acting on the perturbed flat system. The frequency domain developments are crucially facilitated by using a simplified input-to-flat output, additively perturbed, pure integration model of the differentially flat nonlinear system. If the reinterpreted disturbance estimation process is now explicitly used in combination with a ROESO based ADR controller, then, the total disturbance effects on the closed loop system are substantially attenuated in the feedback loop beyond the level achievable by ROESO based ADRC alone. We specifically show that the ROESO based ADRC-DOB combination vastly improves the ESO-based ADR control scheme acting alone, in terms of figures of merit; such as: the Integral Square Error index, obtained for a reference flat output trajectory tracking task. This is done in the context of, both, a simulation example and, experimentally, on a multivariable Permanent Magnet Synchronous Motor platform.

REFERENCES

Chen, W.H. (2004). Disturbance observer based control for nonlinear systems. *IEEE/ASME Transactions on Mechatronics*, 9(4), 706–710.

Chen, W.H., Yang, J., Guo, L., and Li, S. (2016). Disturbance-observer-based control and related methods—an overview. *IEEE Transactions on Industrial Electronics*, 63(2), 1083–1095.

Chiasson, J. (2005). *Modeling and high performance control of electric machines*, volume 26. John Wiley and Sons, Hoboken, New Jersey.

Li, S., Yang, J., Chen, W.H., and Chen, X. (2014). *Disturbance observer-based control: methods and applications.* CRC press (Taylor and Francis Group), Boca Raton, Florida.

Ohishi, K., Nakao, M., Ohnishi, K., and Miyachi, K. (1987). Microprocessor-controlled DC motor for load-insensitive position servo system. *IEEE Transactions on Industrial Electronics*, IE-34(1), 44–49. doi: 10.1109/TIE.1987.350923.

Sira-Ramírez, H., Luviano-Juárez, A., Ramírez-Neria, M., and Zurita-Bustamante, E.W. (2017). *Active disturbance rejection control of dynamic systems: a flatness based approach.* Butterworth-Heinemann, Elsevier, Oxford, UK.

Sira-Ramírez, H., Linares-Flores, J., García-Rodríguez, C., and Contreras-Ordaz, M.A. (2014). On the control of the permanent magnet synchronous motor: An active disturbance rejection control approach. *IEEE Transactions on Control Systems Technology*, 22(5), 2056–2063. doi:10.1109/TCST.2014.2298238.

Sira-Ramírez, H., Zurita-Bustamante, E.W., and Huang, C. (2019). Equivalence among flat filters, dirty derivative-based pid controllers, adrc, and integral reconstructor-based sliding mode control. *IEEE Transactions on Control Systems Technology*, 1–15. doi: 10.1109/TCST.2019.2919822.

Wang, F., Wang, R., Liu, E., and Zhang, W. (2019). Stabilization control mothed for two-axis inertially stabilized platform based on active disturbance rejection control with noise reduction disturbance observer. *IEEE Access*, 7, 99521–99529. doi:10.1109/ACCESS.2019.2930353.

Wang, Y., Tian, D., Dai, M., Shen, H., and Jia, P. (2018). Similarity analysis of disturbance observer and active disturbance rejection control for typical motor-driven system. In *Proc. IEEE 15th Int. Workshop Advanced Motion Control (AMC)*, 132–137. doi: 10.1109/AMC.2019.8371075.

Zurita-Bustamante, E.W., Luviano-Juárez, A., and Sira-Ramírez, H. (2018). On the robust flat-filtering control of mimo nonlinear systems: The pmsm experimental case study. In *June 2018 American Control Conference (ACC)*, 1–4. Milwaukee, WI. doi: 10.23919/ACC.2018.8431316.